RSC Advances

ROYAL SOCIETY OF CHEMISTRY

www.rsc.org/advances

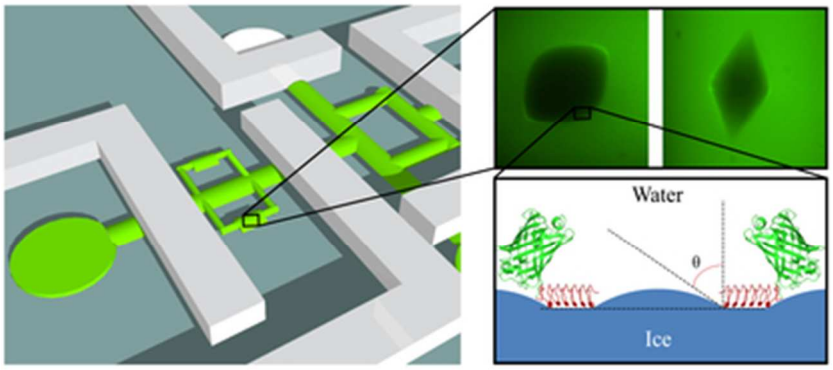

Temperature-controlled microfluidic devices and fluorescence microscopy illustrate the correlation between freezing-point depression and the distance between antifreeze proteins on an ice surface.
35x15mm (300 x 300 DPI)

Journal Name

RSCPublishing

ARTICLE

Experimental Correlation between Thermal Hysteresis Activity and the Distance between Antifreeze Proteins on an Ice Surface

Cite this: DOI: 10.1039/x0xx00000x

Received 00th January 2012,
Accepted 00th January 2012

DOI: 10.1039/x0xx00000x

www.rsc.org/

Ran Drori[a], Peter L. Davies[b], Ido Braslavsky[a]

Antifreeze proteins (AFPs) aid the survival of cold-adapted organisms by inhibiting the growth of ice crystals in the organism. The binding of AFPs to ice separates the melting point from the freezing point of the ice crystal (thermal hysteresis, TH). Although AFPs were discovered more than 40 years ago, the mechanism by which they inhibit ice growth remains unclear. The distance between surface-bound AFPs is thought to correlate directly with the TH activity; however, this correlation has never been experimentally established. A novel microfluidics system was used here to obtain ice crystals covered with GFP-tagged AFPs in an AFP-free solution. This method permits calculation of the surface density of bound AFPs. Fluorescence intensity analysis revealed that the distance between ~3-nm-long AFPs on the ice surface was 7–35 nm, depending on the AFP solution concentration and time of its exposure to ice. A direct correlation between these distances and the measured TH activity was found for a representative insect AFP, but not for a typical fish AFP. Insect AFPs accumulate over multiple ice crystal planes, especially the basal plane. Fish AFPs, which cannot bind to the basal plane, change the shape of the crystal to minimize the basal plane area. Thus, we postulate that the surface density of fish AFPs on the prism plane is not directly indicative of the TH activity, which ends when ice grows out of the basal plane and is a function of the basal plane area. These results significantly contribute to our understanding of the AFP mechanism and will be helpful in applying these proteins in different fields.

1. Introduction

Although antifreeze proteins (AFPs) were discovered more than 40 years ago in fish[1] and later in insects[2], plants[3], fungi[4], and bacteria[5], the exact mechanism by which these proteins bind to ice and inhibit its growth remains unresolved. The cold-adapted organisms mentioned above are able to survive sub-zero environments ranging from –2°C for fish to > –20°C for terrestrial organisms. Applications that take advantage of the AFP properties have tremendous potential. To date, AFPs have been tested as cryosurgery adjuvants[6] and as cryopreservation agents[7]. They have also been incorporated into low-fat ice cream to assist ice structuring[8].

Binding between AFPs and ice separates the melting and freezing temperatures, and the gap between these temperatures is denoted "thermal hysteresis" (TH). The adsorption inhibition model used to explain the AFP effect, proposed by[9], assumes that an AFP molecule bound to an ice surface will not detach from that surface. Experimental evidence supports the irreversible binding between AFPs and ice[10]. AFP binding to an ice surface forces further ice growth to occur only between the surface-bound AFPs. The limited ice growth there increases the local curvature of the ice surface between AFPs and hence decreases the radii of these convex growth areas [9]. The correlation between the surface curvature and the degree of freezing point depression (or TH) is described by the Gibbs–Thomson effect,

$$\Delta T = \frac{2\gamma\Omega Tm}{\rho\Delta H},$$

where γ is the interfacial energy of the ice/water interface, Ω is the molar volume of ice, ρ is the radius of the convex surface, and ΔH is the heat of fusion of water. The Gibbs–Thomson equation describing ice growth in the presence of AFP binding, assuming a distance d = 2ρ between AFP molecules bound to the surface, yields a theoretical value of TH (ΔT). Thus, as the surface density of AFPs increases, the value of ρ decreases, and the non-equilibrium freezing point is further decreased.

We showed recently[11] that two factors influence the TH activity of AFPs in proportion to the surface density of the AFPs: the time period over which a crystal is exposed to the AFPs ("exposure time") and the AFP solution concentration. Increasing the values of these two factors increases the TH activity (although the effects of the exposure time were much more influential in systems involving hyperactive AFPs obtained from insects). Several attempts have been made to measure AFP density on an ice surface. Grandum *et al.* measured the distance between AFPI molecules on the surface of a bipyramidal ice crystal using a scanning tunneling microscope (STM)[12]. They found that the distance between adsorbed AFPI molecules on the pyramidal plane was ~5 nm and the radii of the curved ice surface areas were 2–10 nm. Pertaya *et al.* used fluorescence microscopy to measure the surface densities of the AFPIII-GFP molecules on ice and found that each square micron accommodated 2400 ± 900 AFP molecules when exposed to a solution concentration of 15 ± 5 µM. This surface density corresponded to an average distance of 20 ± 5 nm between AFPIII-GFP molecules[10b]. Zepada *et al.* used fluorescence microscopy to measure the adsorption of FITC-labeled antifreeze glycoproteins (AFGPs) on the non-basal planes of ice crystals. They found that the average spacing between AFGPs was 21 ± 4 nm at a solution concentration of 5 µg/mL [13]. These measurements are consistent with AFP molecules binding within 5–21 nm from one another. Interestingly, the use of these distances (5–21 nm) in the Gibbs–Thomson equation predicts a TH activity 20–5°C, respectively [14]. These predicted TH values are at least one order of magnitude higher than the measured TH activities of the moderate AFPs tested [15]. Values used for the ice surface interfacial energy can vary widely. While Grandum *et al.* used a value of 2 mJ/m^2 to describe the interfacial energy of ice[12], Zepada *et al.* used 30 mJ/m^2 [13]. The distance measurements mentioned above were performed using moderate AF(G)Ps, which cannot bind to the basal plane[11, 15]. Knight and DeVries suggested that AFPs that could not bind to the basal plane minimized the basal plan area so that the TH activity resulted from a limited basal plane area[16]. This suggests that the surface density of a moderate AFP (which is only found on non-basal planes) might not correlate directly with TH activity.

Our objective in this work was to measure the distance between hyperactive AFPs on the surfaces of small ice crystals (similar in size to crystals typically used in the nanolitre osmometer [17]). For the first time, we examined the relationship between these distances and the measured TH activity.

In this report, we exposed ice crystals to hyperactive AFP from *Tenebrio molitor* (*Tm*AFP) and to a moderately active AFP derived from ocean pout (AFPIII), both of which were fused to a green fluorescence protein (GFP). We then measured the fluorescence intensity on the ice surface after removing the AFP-GFP solution. The TH activity of the micron-sized crystals corresponded to the measured distance between the *Tm*AFP-GFP molecules on the ice surface.

2. Experimental

2.1 Antifreeze proteins

Two AFPs fused to GFP were used here: a hyperactive AFP obtained from the common mealworm (*Tenebrio molitor*), *Tm*AFP-GFP[18], stored in a solution containing 20 mM ammonium bicarbonate buffered at pH 8. The second AFP used was the moderate AFPIII derived from ocean pout, AFPIII-GFP[10b], stored in 100 mM ammonium bicarbonate buffered at pH 8.

2.2 Microfluidic system

The microfluidic system used here has been described previously in detail[11]. Briefly, a microfluidic device containing a flow layer for the liquid and an additional layer for the pneumatic valves (fabricated in Dr. Doron Gerber's Lab at Bar Ilan University) was placed on a LabVIEW-controlled cold stage described elsewhere [10a]. The cold stage was mounted on a fluorescence microscope (Ti Eclipse, Nikon, Japan), and a sCMOS camera (Neo 5.5 sCMOS, Andor, UK) was used for video capture and analysis.

A bovine serum albumin (BSA) passivation solution (1% in DDW) was injected to the flow line and left there for 20 min. An ammonium bicarbonate (20 mM) buffer was then injected to remove unbound BSA, and the temperature was lowered until ice crystal nucleation was achieved at –20°C. The temperature was increased toward the bulk melting point until a 50 µm crystal remained. A 980 nm, 500 mW, IR laser (Wuhan Laserlands Laser Equipment Co., ltd, China) was used to melt any unwanted ice crystals in the microfluidic channels. At that point, an AFP-GFP solution was injected into the flow line, and the 50-µm crystal was melted to form a smaller crystal (15–30 µm) in the presence of the AFP-GFP solution. After the crystal had adsorbed AFP-GFP molecules over various exposure time periods, the solution around the crystal was exchanged with a buffer that did not contain AFP-GFP. Next, the temperature was decreased at a fixed rate (0.15°C/min) until crystal growth burst occurred. The difference between the melting point of the crystal and the temperature at which crystal growth burst occurred was defined as the TH activity.

2.3 Calculation of the AFP surface density

The Nis Elements software (Nikon, Japan) was used to measure the fluorescence intensities of the AFP-GFP solution and of the ice crystal surfaces on the non-basal planes. The intensity level in the solution, $I_{solution}$, was proportional to the number of fluorescent molecules present per pixel in the detected volume. The volume that contributed to each pixel extended over the full height of the microfluidic channel. Measurements were performed at the center of the channel, as the flow line of our device was the rounded (see Supplementary Information S1 and in reference 11). The number of fluorescent molecules present in this volume was equal to this volume multiplied by the solution concentration, C. Thus the intensity $I_{solution} = h(\mu m) * A * C(\mu M) * I_0$, where h is the height of the channel, A is an area unit in the sample that contributed to the intensity of a given pixel in the camera, C is the concentration of the fluorescence molecules, and I_0 is the fluorescence signal per molecule for a given illumination and detection setting.

The intensity measured on the ice surfaces, I_{ice}, was proportional to the surface density of AFP-GFP molecules multiplied by 2, to take into account the two side of the crystal (as these crystals are transparent, the measured intensity on the surface was the sum of the densities on the bottom and top sides of the crystal). Thus,

$$I_{ice} = 2 * A * \sigma(\frac{molecules}{\mu m^2}) * I_0,$$

where A is the area unit in the sample that contributed to the intensity for a given pixel in the camera, σ is the surface density of the AFP molecules on the ice surface, and I_0 is the fluorescence signal per molecule under given illumination and detection conditions.

The ratio of the two intensities yielded

$$\frac{I_{solution}}{I_{ice}} = \frac{20(\mu m)*C(\mu M)}{2*\sigma(\frac{molecules}{\mu m^2})}.$$

The value of σ (number of AFP-GFP molecules per µm^2) was calculated according to

$$\sigma = \frac{I_{ice}}{I_{solution}} * \frac{20(\mu m)C(\mu M)}{2},$$

and the average distance between AFP-GFP molecules could be obtained using the equation

$$d = \sqrt{\frac{1}{\sigma}}.$$

For example, if $\frac{I_{ice}}{I_{solution}} = 0.1$ and $C = 10\ \mu M$, then

$$\sigma = 0.1 * \frac{1}{2} * 20(\mu m) * 10^{-5}(M) * 6.022 * 10^{23}\left(\frac{molcules}{mole}\right) * \left(\frac{mole}{Liter} * \frac{1}{M}\right) * \left(\frac{Liter}{10^{15}\mu m^3}\right),$$

$\sigma = 6{,}000\frac{molcules}{\mu m^2}$ and d = 13 nm average distance between molecules.

3. Results and discussion

The distance between AFPs on the ice surface was measured by calculating the surface density of the AFP-GFP molecules on the ice crystals using fluorescence microscopy (see the Experimental section for details about the calculation). It was shown earlier that tagging an AFP with a GFP molecule increases the TH activity[10b, 19], and the kinetics of the TH were shown to be similar for both GFP-tagged and untagged *Tm*AFP[11]. Pertaya *et al*. showed that GFP molecules did not bind to ice by analyzing the intensity levels of free GFP near ice crystals. This analysis was done by comparing the intensity level of GFP to Cy5 dye molecule that cannot bind to ice. The intensity levels of Cy5 and free GFP were similar and unlike the GFP-AFP conjugates that show clear differences from the Cy5 dye[10b]. This evidence shows that GFP by itself has no measurable effect on our results.

Next, the TH activity of these crystals was measured. Each crystal was exposed to an AFP-GFP solution at a different concentration and exposure time[11] (Supplementary information S2 and S3), then the AFP-GFP solution was removed and the TH activity was measured. By removing the AFP-GFP solution, we experimentally removed the contribution of the solution fluorescence to the measured intensity, unlike the mathematical correction implemented by Pertaya *et al.*[10b] and by Zepeda *et al.*[13] in which the intensity from the area near the crystal was corrected by using the intensity from the solution away from the crystals.

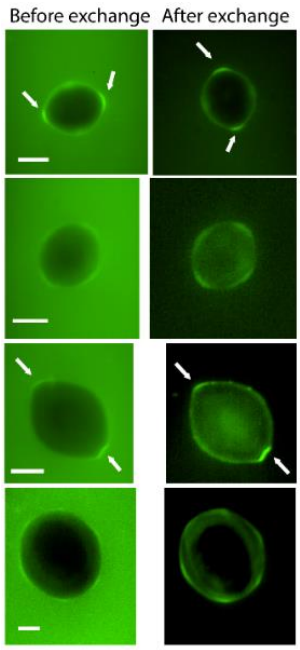

Figure 1 - Ice crystals before and after *Tm*AFP solution exchange. The crystals were incubated in *Tm*AFP-GFP solutions for different time periods, after which the protein solution was removed. The brighter areas in some of the images denote AFP adsorption on the basal plane of the crystal (white arrows). Size bar is 10 µm.

In our experiments the fluorescence intensity was measured on the non-basal planes of the crystal to avoid saturation readings in our measurements, as the basal planes of most crystals (Figure 1) were characterized by high intensity levels as a result of the parallel orientation of the crystals basal plane compare to the optical axis of the illumination (see reference 11 for more details). Another aspect we considered is the possibility of having AFP-GFP trapped within the ice. Such incorporation occurs when ice is growing in the presence of AFP-GFP during the initial freezing of the sample. To avoid AFP-GFP inside the ice crystals, we first froze the entire sample, and then melted the bulk ice to obtain an ice crystal of ~40 µm in size. Then, the AFP-GFP solution was introduced, and AFP-GFP molecules could bind to the outer surface of the crystal. Further details can be found in reference 11**.** To avoid false measurements of the surface density, we only used ice crystals nucleated in solutions that did not contain AFP-GFP.

We found that the average distances between the surface-bound *Tm*AFP-GFP molecules (Figure 2) were 7–35 nm, depending on the AFP solution concentration and the exposure time. The values were similar to those reported previously using AFPIII-GFP[10b], 20 ± 5 nm, or using FITC-labeled AFGPs[13], 21 ± 4 nm, and were at the high end for measurements made on AFPI[12]. These measured distances, however, were not correlated with the TH activity measurements of the micron-sized crystals used in typical TH activity measurements[17]. The average values of the distance between AFPs were plotted against the measured TH activity for each crystal (Figure 2 and Supplementary information S4).

As predicted by the Gibbs–Thomson framework shown in the introduction section, the TH increased as the distance between AFPs on the ice surface decreased. We next inverted the distances to obtain the inverted relationship (from the Gibbs–Thomson equation)

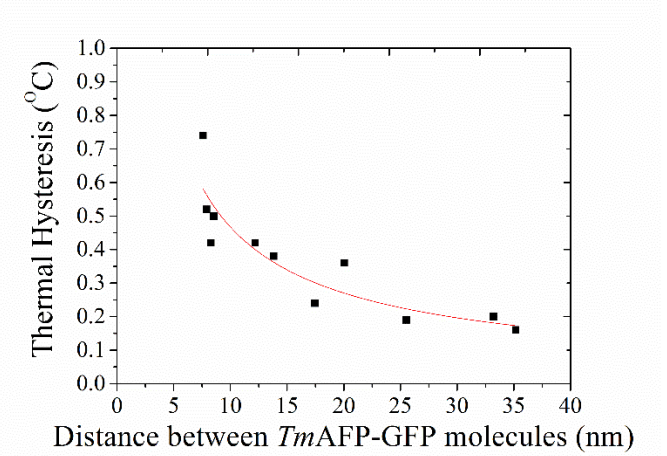

Figure 2 – TH activity as a function of the average distance between *Tm*AFP-GFP molecules on the ice surfaces. The distance between AFPs on the ice surfaces was calculated as discussed in the Materials and Methods Section. Each data point was obtained from a crystal that had adsorbed *Tm*AFP-GFP molecules from a different solution concentration over a different time period. The TH activity was measured after the AFP solution had been removed.

between TH and the radius of the curved interface. Figure 3 plots the relationship between the inverted distance between AFPs and TH activity. This relationship was found to be linear. These results indicated that the TH activity was indeed correlated with the distance between AFPs. The effect of the surface density for moderate AFPIII-GFP on the TH activity was investigated by measuring the distance between the AFPs on the ice surface and the TH activity using the method applied to the *Tm*AFP-GFP studies. We found that the distances between AFPIII-GFP molecules on the ice surface were 8–25 nm. These values were similar to the distances obtained in previous studies of moderate AFPs[10b, 12-13] and in our own measurements of hyperactive *Tm*AFP-GFP.

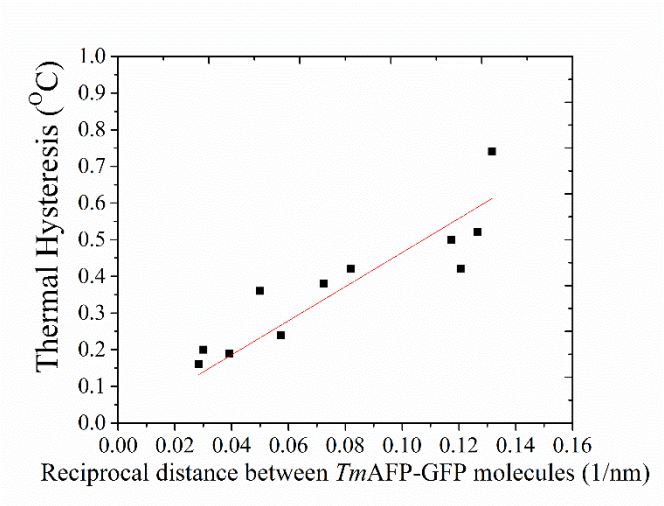

Figure 3 – TH activity as a function of the reciprocal distance between *Tm*AFP-GFP molecules on the ice surfaces. The linear relationship of distance between *Tm*AFP-GFP molecules and TH activity was obtained by plotting the reciprocal of the distance between surface-bound AFPs. The fit formula is $TH = \frac{4.6\,nm\,K}{d}$. The R-squared value of this curve is 0.78.

In contrast with the *Tm*AFP-GFP distance measurements (Figure 2), no convincing correlations were found between the measured TH and the distance between the AFPIII-GFP proteins on the ice surface (Figure 4). Thus, the surface density of the moderate AFPs did not directly affect the TH activity. The significance of these results is discussed below.

This report describes the first surface density measurements performed using a hyperactive AFP and the first experimental correlation to the measured TH activity. To date, all measurements of the AFP ice surface density have been performed using moderate AFPs[10b, 12-13] that cannot bind to the basal plane[11, 15]. Here we showed that the ice surface density of the moderately active AFPIII was not correlated with the TH activity. This observation led us to hypothesize that TH is not a direct result of the inter-AFP distance for moderate AFPs, and the surface density is not the only parameter that governs TH. Hence, any attempt to predict the TH activity based on the distance between moderate AFPs must account for other factors, including the size of the basal plane[16].

Hyperactive AFPs bind to many crystal planes, including the basal plane[11]; thus the surface density directly affects the TH activity. Our results obtained from AFP ice surface density measurements agreed with previous reports[10b, 12-13] that examined different types of AF(G)P with inter-protein distances between 2 and 21 nm. Substituting our results into the Gibbs–Thomson equation yielded a predicted TH activity that was one order of magnitude higher than our measured TH activity, as has been observed previously[13]. The discrepancies between the theoretical model and the experimental results may potentially be explained in terms of the factors proposed by [20] and [14],

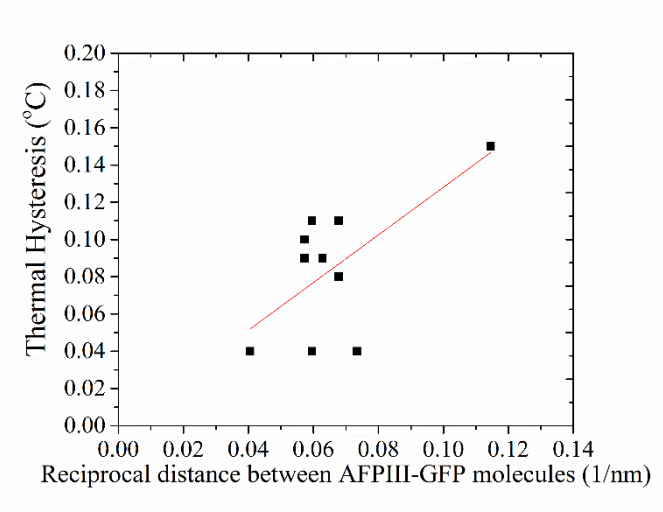

Figure 4 – TH activity as a function of the reciprocal distance between AFPIII-GFP molecules present on the ice surfaces. The distances between AFPs on the ice surfaces were calculated, as discussed in the Experimental section. Each data point was obtained from a crystal that had adsorbed AFPIII-GFP molecules from a different solution concentration. The TH activity was measured after the AFP solution had been removed or during solution exchange. The linear relationship of the distance between AFPIII-GFP molecules was obtained by plotting the reciprocal of the distance between surface-bound AFPs. Fitting to a linear curve that intercepts with zero has a low R-squared value of 0.39.

who studied ice growth in restricted areas. Higgins and Karlsson recently examined intracellular ice formation (IIF) in mouse insulinoma cells[21]. They postulated that ice growth between cells occurred so as to maintain a certain contact angle, θ, between the ice/water interface and the pore wall. The value of cos θ must be considered in any description of the effects of the ice surface curvature on the freezing point depression. The angles that fitted their data were 69.1±1.3° for the gap junctions (with ~3 nm between cells), and 86.6±0.2° for the tight junctions (with ~0.5 nm diameter pores). Theoretical treatments of the contact angle have been discussed elsewhere in the AFP field[22].

We suggested using the following revised Gibbs–Thomson equation:

$\boldsymbol{TH = \frac{4\Omega\gamma T_m \cos\theta}{\Delta H d}}$, where d is the distance between AFPs, θ is the contact angle shown in Figure 5, Ω is the molar volume of ice, γ is the interfacial energy, ΔH is the latent heat, and T_m is the bulk melting point. Our measurements of the distance between AFPs and the TH were used to find that θ should be 85±1°. This value corresponded with previous similar measurements[21]. A cartoon describing our interpretation of the binding properties of *Tm*AFP-GFP is shown in Figure 5. We note that GFP is a big marker molecule (27 kD) and it can in principle influence the results compare to non-labeled *Tm*AFP

(9 kD). Previously it was found that theTH of AFP-GFP was slightly increased compared to AFP at the same molar concentrations[11]. It is possible that the GFP tag influences the relationship between surface density and TH, in particularly at close proximity where the distance between molecules approaches the size of these molecules. This influence could shift the nominal measured distance between AFPs. However, our conclusion that for hyperactive AFPs there is a correlation between TH and the measured surface density still remains. For the same concentration, the TH of untagged AFP[11] is lower compared to GFP-tagged AFP, thus if the average distance is similar, the discrepancy with the Gibbs-Thomson equation would increase.

A large contact angle (θ in Figure 5) might indicate an influence of the protein on the interface between ice and water. Recently it was found by terahertz measurements that the structure of the water network is influenced by AFPs over more than a nanometer from the AFP surface[23]. Also, in a molecular dynamics simulation it was found that AFPs could locally melt thin ice crystals slab[24]. Although these findings need further verification they add to the interest in the influence of AFPs on the ice-water interface. Inclusion of the contact angle in the Gibbs–Thomson equation may address the significant inconsistencies observed in previous surface density measurements and the calculated TH activity discussed in reference13.

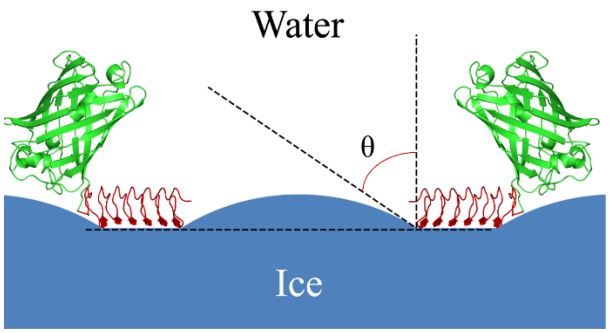

Figure 5 – The local ice surface curvature as a result of binding by *Tm*AFP-GFP molecules through a contact angle θ. The red structure flush with the ice surface is *Tm*AFP. The attached green barrel is GFP.

4. Conclusions

In summary, we demonstrated that the ice surface protein density of *Tm*AFP, a representative hyperactive AFP that binds to multiple ice planes, correlates with its TH activity[11]. This correlation was not observed for the moderately active AFPIII, which cannot bind to the basal plane[11]. Moderate AFPs minimize the basal plane area when the ice crystal grows into its bipyramidal shape. Thus, the surface densities of the moderate AFPs are not the only parameters that determine TH. The basal plane size also plays a role[16]. For the hyperactive AFP, the TH values were smaller than expected from the Gibbs-Thomson equation. Thus, we proposed a revised Gibbs–Thomson equation that considers the contact angle formed by the local curvature of the ice crystal surface. This modification suggests that the AFPs influence their immediate water environments, as suggested previously[23, 25]. Our results indicate that the TH is correlated to distance between hyperactive AFPs, and in addition that the bound proteins may change the local surface tension of the ice water interface.

Acknowledgements

Supported by the European Research Council (ERC), The Israel Science Foundation (ISF), Canadian Institutes of Health Research (CIHR), the Lady Davis Foundation, and the Canada Research Chair program.

Notes and references

[a]Institute of Biochemistry, Food Science and Nutrition, The Robert H. Smith Faculty of Agriculture, Food and Environment , The Hebrew University of Jerusalem, Rehovot, Israel. [b]Department of Biomedical and Molecular Sciences, Queen's University, Kingston, ON, Canada.

1. DeVries, A. L., Glycoproteins as biological antifreeze agents in antarctic fishes. *Science* **1971,** *172* (988), 1152-5.
2. Tomchaney, A. P.; Morris, J. P.; Kang, S. H.; Duman, J. G., Purification, composition, and physical properties of a thermal hysteresis "antifreeze" protein from larvae of the beetle, Tenebrio molitor. *Biochemistry* **1982,** *21* (4), 716-21.
3. Urrutia, M. E.; Duman, J. G.; Knight, C. A., Plant thermal hysteresis proteins. *Biochim Biophys Acta* **1992,** *1121* (1-2), 199-206.
4. Robinson, C. H., Cold adaptation in Arctic and Antarctic fungi. *New Phytol* **2001,** *151* (2), 341-353.
5. Sun, X.; Griffith, M.; Pasternak, J. J.; Glick, B. R., Low temperature growth, freezing survival, and production of antifreeze protein by the plant growth promoting rhizobacterium Pseudomonas putida GR12-2. *Can J Microbiol* **1995,** *41* (9), 776-84.
6. Pham, L.; Dahiya, R.; Rubinsky, B., An in vivo study of antifreeze protein adjuvant cryosurgery. *Cryobiology* **1999,** *38* (2), 169-75.
7. (a) Beirao, J.; Zilli, L.; Vilella, S.; Cabrita, E.; Schiavone, R.; Herraez, M. P., Improving sperm cryopreservation with antifreeze proteins: effect on gilthead seabream (Sparus aurata) plasma membrane lipids. *Biology of reproduction* **2012,** *86* (2), 59; (b) Carpenter, J. F.; Hansen, T. N., Antifreeze protein modulates cell survival during cryopreservation: mediation through influence on ice crystal growth. *Proc Natl Acad Sci U S A* **1992,** *89* (19), 8953-7.
8. (a) Clarke, C. J.; Buckley, S. L.; Lindner, N., Ice structuring proteins - a new name for antifreeze proteins. *Cryo Letters* **2002,** *23* (2), 89-92; (b) Regand, A.; Goff, H. D., Ice recrystallization inhibition in ice cream as affected by ice structuring proteins from winter wheat grass. *J Dairy Sci* **2006,** *89* (1), 49-57.
9. Raymond, J. A.; DeVries, A. L., Adsorption inhibition as a mechanism of freezing resistance in polar fishes. *Proc Natl Acad Sci U S A* **1977,** *74* (6), 2589-93.
10. (a) Celik, Y.; Drori, R.; Pertaya-Braun, N.; Altan, A.; Barton, T.; Bar-Dolev, M.; Groisman, A.; Davies, P. L.; Braslavsky, I., Microfluidic experiments reveal that antifreeze proteins bound to ice crystals suffice to prevent their growth. *Proc Natl Acad Sci U S A* **2013,** *110* (4), 1309-14; (b) Pertaya, N.; Marshall, C. B.; DiPrinzio, C. L.; Wilen, L.; Thomson, E. S.; Wettlaufer, J. S.; Davies, P. L.; Braslavsky, I., Fluorescence microscopy evidence for quasi-permanent attachment of antifreeze proteins to ice surfaces. *Biophys. J.* **2007,** *92* (10), 3663-3673.
11. Drori, R.; Celik, Y.; Davies, P. L.; Braslavsky, I., Ice-binding proteins that accumulate on different ice crystal planes produce distinct thermal hysteresis dynamics. *Journal of the Royal Soceity Interface* **2014**.

12. Grandum, S.; Yabe, A.; Nakagomi, K.; Tanaka, M.; Takemura, F.; Kobayashi, Y.; Frivik, P. E., Analysis of ice crystal growth for a crystal surface containing adsorbed antifreeze proteins. *J Cryst Growth* **1999,** *205* (3), 382-390.
13. Zepeda, S.; Yokoyama, E.; Uda, Y.; Katagiri, C.; Furukawa, Y., In situ observation of antifreeze glycoprotein kinetics at the ice interface reveals a two-step reversible adsorption mechanism. *Cryst Growth Des* **2008,** *8* (10), 3666-3672.
14. Liu, Z.; Muldrew, K.; Wan, R. G.; Elliott, J. A., Measurement of freezing point depression of water in glass capillaries and the associated ice front shape. *Phys Rev E Stat Nonlin Soft Matter Phys* **2003,** *67* (6 Pt 1), 061602.
15. Scotter, A. J.; Marshall, C. B.; Graham, L. A.; Gilbert, J. A.; Garnham, C. P.; Davies, P. L., The basis for hyperactivity of antifreeze proteins. *Cryobiology* **2006,** *53* (2), 229-39.
16. Knight, C. A.; DeVries, A. L., Ice growth in supercooled solutions of a biological "antifreeze", AFGP 1-5: an explanation in terms of adsorption rate for the concentration dependence of the freezing point. *Phys Chem Chem Phys* **2009,** *11* (27), 5749-5761.
17. Braslavsky, I.; Drori, R., LabVIEW-operated Novel Nanoliter Osmometer for Ice Binding Protein Investigations. *J. Vis. Exp.* **2013,** *72*.
18. Bar, M.; Bar-Ziv, R.; Scherf, T.; Fass, D., Efficient production of a folded and functional, highly disulfide-bonded beta-helix antifreeze protein in bacteria. *Protein Expr Purif* **2006,** *48* (2), 243-52.
19. DeLuca, C. I.; Comley, R.; Davies, P. L., Antifreeze proteins bind independently to ice. *Biophys J* **1998,** *74* (3), 1502-8.
20. Mazur, P., The role of cell membranes in the freezing of yeast and other single cells. *Annals of the New York Academy of Sciences* **1965,** *125* (2), 658-76.
21. Higgins, A. Z.; Karlsson, J. O., Effects of intercellular junction protein expression on intracellular ice formation in mouse insulinoma cells. *Biophys J* **2013,** *105* (9), 2006-15.
22. (a) Knight, C. A.; Cheng, C. C.; DeVries, A. L., Adsorption of alpha-helical antifreeze peptides on specific ice crystal surface planes. *Biophys J* **1991,** *59* (2), 409-18; (b) Kristiansen, E.; Ramlov, H.; Hagen, L.; Pedersen, S. A.; Andersen, R. A.; Zachariassen, K. E., Isolation and characterization of hemolymph antifreeze proteins from larvae of the longhorn beetle Rhagium inquisitor (L.). *Comparative biochemistry and physiology. Part B, Biochemistry & molecular biology* **2005,** *142* (1), 90-7.
23. Meister, K.; Ebbinghaus, S.; Xu, Y.; Duman, J. G.; DeVries, A.; Gruebele, M.; Leitner, D. M.; Havenith, M., Long-range protein-water dynamics in hyperactive insect antifreeze proteins. *Proc Natl Acad Sci U S A* **2013,** *110* (5), 1617-22.
24. (a) Calvaresi, M.; Hofinger, S.; Zerbetto, F., Local ice melting by an antifreeze protein. *Biomacromolecules* **2012,** *13* (7), 2046-52; (b) Todde, G.; Whitman, C.; Hovmoller, S.; Laaksonen, A., Induced Ice Melting by the Snow Flea Antifreeze Protein from Molecular Dynamics Simulations. *J Phys Chem B* **2014**.
25. Siemer, A. B.; Huang, K. Y.; McDermott, A. E., Protein-ice interaction of an antifreeze protein observed with solid-state NMR. *Proc Natl Acad Sci U S A* **2010,** *107* (41), 17580-5.

